Atmospheric Environment 277 (2022) 119063

Contents lists available at ScienceDirect

Atmospheric Environment

journal homepage: www.elsevier.com/locate/atmosenv

Sensitivity of total column NO_2 at a marine site within the Chesapeake Bay during OWLETS-2

Alexander Kotsakis [a,b,1,*], John T. Sullivan [b], Thomas F. Hanisco [b], Robert J. Swap [b], Vanessa Caicedo [g,h], Timothy A. Berkoff [c], Guillaume Gronoff [c,d], Christopher P. Loughner [e], Xinrong Ren [e,f], Winston T. Luke [e], Paul Kelley [e,f], Phillip R. Stratton [f], Ruben Delgado [g,h], Nader Abuhassan [b,g], Lena Shalaby [b,g], Fernando C. Santos [i], Joel Dreessen [j]

[a] Universities Space Research Association, Columbia, MD, USA
[b] NASA Goddard Space Flight Center, Greenbelt, MD, USA
[c] NASA Langley Research Center, Hampton, VA, USA
[d] Science Systems and Applications Inc., Hampton, VA, USA
[e] Air Resources Laboratory, National Oceanic and Atmospheric Administration, College Park, MD, USA
[f] University of Maryland, College Park, MD, USA
[g] Joint Center for Earth Systems Technology, Baltimore, MD, USA
[h] University of Maryland Baltimore County, Baltimore, MD, USA
[i] Boston University, Boston, MA, USA
[j] Maryland Department of the Environment, Baltimore, MD, USA

HIGHLIGHTS

- Clustered back trajectories showed that westerly & northwesterly winds resulted in the highest ozone values.
- TROPOMI captured the spatial variability of NO_2 observed by the Pandora network, including accumulation of NO_2 over water.
- Configuration of O_3 lidar, Pandora, wind lidar, and in situ measurements, detected lofted plumes of NO_2 and O_3 over water.

ARTICLE INFO

Keywords:
Pandora
Ozone lidar
Wind lidar
Chesapeake Bay
Back trajectory model
Nitrogen dioxide
Ozone

ABSTRACT

In coastal environments like the Chesapeake Bay, the presence of the sea/bay breeze circulation can contribute to poor air quality and makes modeling the meteorological and chemical impacts of the sea/bay breeze in air quality forecast models a challenge. The Ozone Water-Land Environmental Transition Study 2 field campaign aimed to better quantify the mechanisms affecting surface, profile, and columnar trace gas amounts between the land and water. Using HYSPLIT back trajectory modeling, the meteorological variability affecting Pandora NO_2 and surface O_3 was quantified. Clustered back trajectories showed that westerly and north-northwesterly winds resulted in the highest MDA8 ozone values over the study domain. An analysis of multiday ozone event, demonstrated how TROPOMI can capture the spatial variability of NO_2 observed by the Pandora network, including the accumulation of NO_2 over the Chesapeake Bay. VOC measurements during multiday ozone event were analyzed and sources of ozone precursors, such as a coal fire power plant, were identified. Further investigation of the surface ozone data at HMI revealed that significant amounts of ozone were maintained over the Chesapeake Bay at night. Using a combination of ozone lidar, Pandora, in situ O_3 and NO_2, and wind lidar measurements, a lofted plume of NO_2 was detected over water. Additionally, the same suite of observations found significant differences in the horizontal and vertical extent of ozone on the highest exceedance day of the event. Surface measurements of trace gases (NO_2 and O_3) can vary significantly from remote sensing (Pandora, TROPOMI, O3lidar), highlighting the need for sensitive profile, columnar, and in situ measurements in complex urban, marine environments for future geostationary air quality validation.

* Corresponding author. Universities Space Research Association, Columbia, MD, USA.
E-mail address: alexander.e.kotsakis@nasa.gov (A. Kotsakis).
[1] Now at: ERT, Inc., Laurel, MD, 20707, USA.

https://doi.org/10.1016/j.atmosenv.2022.119063
Received 25 October 2021; Received in revised form 14 February 2022; Accepted 13 March 2022
Available online 21 March 2022

1. Introduction/background

Tropospheric ozone (O_3) and nitrogen dioxide (NO_2) significantly impact air quality and climate. NO_2 can impact human respiratory health (Peel et al., 2005) and is the primary precursor species for photochemical ozone production, nitrate aerosol formation, and impacts the abundance of hydroxyl radicals (OH) and lifetimes of numerous greenhouse gases (Solomon, 1999). Ozone, a strong greenhouse gas and the primary constituent of photochemical smog, can negatively impact human respiratory health and lead to vegetative stress (Avnery et al., 2011; Lefohn and Foley, 1993). Historically, pollutant characterizations have been well studied using continental monitoring sites. However, chemical transport and the land-water interface impacts on pollutants and emissions continue to need further investigation (Sullivan et al., 2019).

The vertical and spatial abundance of these trace gases can be impacted by meteorological transport, photochemistry, emissions, and mixing within the boundary layer (Sullivan et al., 2017). One of the extensively researched meteorological factors that can affect vertical and spatial abundance of these trace gases along urban coastlines is a mesoscale feature known as the sea, bay, or lake breeze. Sea, bay, or lake breezes form due to the different thermal gradients at land-water interfaces, resulting in a land breeze (offshore flow) during the overnight hours and a sea/bay/lake breeze (onshore flow) during the afternoon hours. Ozone exceedances in coastal urban areas are often associated with the presence of a sea, bay, or lake breeze circulation (Banta et al., 2005, 2011; Caicedo et al., 2019; Li et al., 2020; Loughner et al., 2011, 2014; Rappenglück et al., 2008; Ryu et al., 2013; J. Zhang et al., 2020) and contribute to substantial increases in surface ozone in the late afternoon. In coastal environments like the Chesapeake Bay, the presence of the bay breeze circulation contributes to poor air quality (Knepp et al., 2015; Stauffer et al., 2015) and modeling the meteorological and chemical impacts of the sea breeze in air quality forecast models is a challenge (Goldberg et al., 2014; Loughner et al., 2011).

Remote sensing measurements of NO_2 from space (e.g., Ozone Monitoring Instrument (OMI)) historically have not had the spatial resolution to effectively resolve small scale trace gas gradients induced by sea/bay/lake breeze boundaries. The largest source of uncertainty in OMI NO_2 retrievals is the profile shape within the air mass factor (AMF) calculation (Boersma et al., 2004; Lorente et al., 2017). The accuracy of the shape profile can significantly affect the amount of satellite retrieved NO_2 and is sensitive to the resolution of the chemical transport model used to determine the shape profiles (Goldberg et al., 2017; Lamsal et al., 2014). Based on data from the Deriving Information on Surface conditions from Column and Vertically Resolved Observations Relevant to Air Quality (DISCOVER-AQ) field campaigns, which were aimed at better resolving trace gas profile variability, the variability of NO_2 and O_3 profiles can be significantly affected by atmospheric stability (Y. Zhang et al., 2016) and chemistry (He et al., 2013). Flynn et al. (2016) also found that depending on the amount of vertical mixing, urban setting, and time of the year, the amount of observed NO_2 and O_3 profile variability can vary.

To better understand pollutant transport and photochemical production of ozone, it is critical to understand the spatial and temporal variability of its primary precursor, NO_2. Over the last decade, an easily deployable ground-based spectrometer instrument called Pandora has been frequently utilized in satellite validation and field campaigns by providing direct sun column measurements of NO_2 and O_3 at high temporal resolution (Herman et al., 2009). In previous comparisons of OMI and Pandora, column NO_2 measured from OMI was typically biased low compared to Pandora in urban areas due to the relatively coarse spatial resolution of OMI, measurement location, uncertainty in the air mass factor calculation, and heterogeneous nature of NO_2 (Herman et al., 2018; Kim et al., 2016). However, this bias is reduced with the improved spatial resolution of the recently launched TROPOspheric Monitoring Instrument (TROPOMI) instrument (Griffin et al., 2019; Ialongo et al., 2020; Judd et al., 2019; Zhao et al., 2020). The next-generation air quality monitoring satellites will provide a unique perspective by making measurements from geostationary orbit (Fishman et al., 2008). The Tropospheric Emissions: Monitoring of Pollution (TEMPO) satellite (Zoogman et al., 2017), which will have a comparable spatial resolution to TROPOMI, will provide daytime, hourly measurements of total column (TC) O_3 and NO_2, tropospheric O_3 and NO_2, and 0–2 km and 10–20 km O_3 across North America starting in early 2023. Properly quantifying the covariance of surface concentrations, trace gas profiles, and column amounts simultaneously at land-water interfaces is critical for accurate, hourly trace gas retrievals from space.

The Ozone Water-Land Environmental Transition Study (OWLETS) was carried out to specifically quantify the spatial and vertical distribution of trace gases around the Chesapeake Bay and better connect ground-level pollutant concentrations to satellite measurements. The first iteration of OWLETS (Sullivan et al., 2019) was carried out in the southern Chesapeake Bay during the summer of 2017, while the second iteration (OWLETS-2) took place in the northern part of the Chesapeake Bay close to the DC-Baltimore metropolitan area during the summer of 2018. The unique characteristic of the OWLETS campaigns was the presence of a heavily instrumented site within the Chesapeake Bay on a remote island and adjacent traditional continental monitoring sites (Fig. 1). Measurements from this island site could be contrasted to observations on land to observe how trace gas gradients were captured by ground-based and space-based measurements, while simultaneously observing the mesoscale meteorology (i.e., bay breeze) affecting these chemical gradients. As the first major field campaign to revisit the study area since DISCOVER-AQ Maryland in 2011, OWLETS-2 provided an opportunity to analyze how any chemical and meteorological mechanisms have changed within the Chesapeake Bay airshed and take advantage of the, at the time, newly available TROPOMI measurements.

In this study, we utilized data from the OWLETS-2 campaign to evaluate column NO_2 gradients using Pandora measurements and analyzed these gradients to determine if they could be detected by TROPOMI. These ground-based and satellite remotely sensed NO_2 gradients were further contextualized by utilizing a meteorological back trajectory model and analyzing ground-level ozone concentrations. Finally, using a combination of in situ, ozone lidar, doppler wind lidar, Pandora, and TROPOMI measurements, a unique weekend ozone event was analyzed to further contextualize the relationship between remotely sensed NO_2 and ozone concentrations over the bay. The results of this work demonstrate the ability of higher resolution satellite measurements to effectively capture NO_2 gradients at land-water interfaces and how multiple ground-based remote sensing platforms can be integral to disentangling the diurnal and vertical variability of NO_2 and O_3 over coastal regions.

2. Data and methods

The OWLETS-2 field campaign utilized an array of ground sites that was complemented by aircraft measurements. The ground and aircraft assets featured both in situ and remote sensing trace gas measurements (Fig. 1). The campaign specific air quality monitoring ground sites were located across the Baltimore area with some already existing Maryland Department of Environment (MDE) and Environmental Protection Agency (EPA) sites being utilized. Two of the unique and well instrumented sites were Hart Miller Island (HMI), which is located directly east of Baltimore in the Chesapeake Bay, and the University of Maryland – Baltimore County (UMBC), which is located in southwest Baltimore. The main goal of this work is to illustrate how the instrumentation at HMI and UMBC were able to capture the chemical differences between "over water" and "over land", especially during the presence of land-sea/bay breeze circulations. The data utilized from the array of sites in the study area is described below:

2.1. Pandora

The Pandora spectrometer instrument is a ground-based UV-VIS remote sensing instrument that provides high temporal resolution operational retrievals of O_3 and NO_2 using differential optical absorption spectroscopy (DOAS) (Herman et al., 2009). This instrument can operate in direct-sun and sky scanning modes to provide columnar and profile measurements, respectively. Under a traditional direct sun operation schedule and using, Pandora provides a new data point for total column (TC) NO_2 and O_3 approximately every 120 s. For the retrieval of NO_2, a spectral fitting algorithm was applied using spectra collected close to solar noon from which the slant column amounts can be derived (Herman et al., 2009). Slant to vertical column conversion was performed using a geometric air mass factor (AMF) since the majority of path length is dominated by direct solar beams, rather than scattered light (Cede, 2019). For the purposes of this study, the direct sun total column NO_2 is used for all sites analyzed. The stated accuracy of the operational direct sun total column NO_2 algorithm is 0.05 Dobson unit, or DU (2.7×10^{15} molecules cm^{-2}) and a precision of 0.002 DU (5.3×10^{13} molecules cm^{-2}) (Cede, 2021).

All Pandora datasets were filtered using Data Quality Flags (DQF) provided in the L2 data file. These data quality flags represent a composite of uncertainty, signal to noise, and AMF thresholds. Only data with 0, 1, 10, or 11 DQF were used in this study as these represent data with either high or medium quality data. While improvements are still being made to the DQF criteria, some data points with values below 0.1 DU remained in the dataset. Since total column values of $\leq$0.1 DU are even less than stratospheric column NO_2 amounts, these values are not realistic. Due to this, additional filtering was performed to not include data points below 0.1 DU. Only one site had a data file with no DQFs due to the data being collected on the previous Pandora operation and processing software (PanOS). These data were filtered to only include data with normalized root mean squared error of <0.01 and total column uncertainty <0.05 DU. For this study, NASA owned Pandora instruments were set up at the University of Maryland Baltimore County (Pandora #19), Howard University Beltsville (Pandora #18), Earth System Science Interdisciplinary Center (Pandora #21), Research Vessel (Pandora #24) and Hart Miller Island (Pandora #26 and #30). Each of these instruments were operated in direct sun mode to enable comparisons between satellite (e.g., OMI and TROPOMI) and aircraft remote sensing (e.g., GeoTASO) measurements. These Pandoras were operated from approximately June–August 2018.

2.2. TROPOMI

The TROPOspheric Monitoring Instrument (TROPOMI) onboard the Sentinel 5-P satellite, was launched on October 13, 2017, and has been providing global, high spatial resolution trace gas measurements on a daily basis since May 2018. TROPOMI is a passive nadir viewing satellite borne push-broom imaging spectrometer with 8 spectral bands in the UV, VIS, near infrared (NIR) and short-wavelength infrared (SWIR). TROPOMI has a local overpass time of ~13:30 LT and a ground pixel size of 3.5 km (across-track) x 7.0 km (along-track). Recent changes to the operating scenario on August 6, 2019 have resulted in a higher spatial resolution of 3.5 km (across-track) x 5.5 km (along track). The TROPOMI NO_2 retrieval algorithm requires using a 3-dimensional global Tracer Model 5 (TM5) chemistry transport model (CTM) (Williams et al., 2017). The retrieval process is broken down into a three-step process with the outcome being tropospheric, stratospheric, and total column densities. The total NO_2 slant column densities are retrieved using Level-1b radiance and irradiance spectra measured by TROPOMI through the differential optical absorption spectroscopy (DOAS) approach. Using data assimilated from the Tracer Model 5 Massively Parallel (TM5-MP) CTM (Williams et al., 2017), the tropospheric and stratospheric NO_2 column densities are able to be separated. The tropospheric and stratospheric slant column densities are then converted to vertical densities using air mass factors (AMF) from a look-up table of altitude dependent AMFs and daily vertical distributions of NO_2 from the TM5-MP model. To analyze the spatial heterogeneity of NO_2 during the OWLETS-2 campaign period, L2 Tropospheric Column NO_2 overpass data was analyzed for each day.

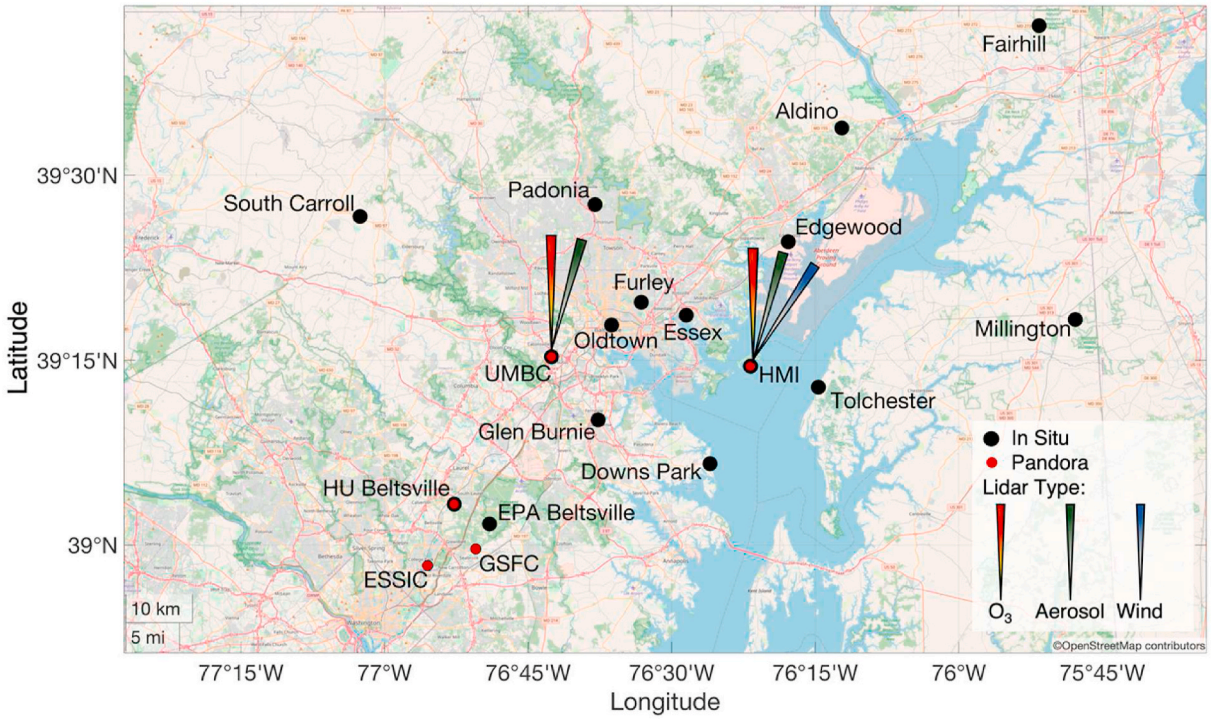

Fig. 1. Map of OWLETS-2 sites that had Pandora instruments (red dots), in situ trace gas measurements (black dots), and lidar measurements (vertical cones). The type of lidars at a site are depicted by the clockwise orientation of the cones (ozone – aerosol – wind). (For interpretation of the references to color in this figure legend, the reader is referred to the Web version of this article.)

The L2 data used in this study is the offline version (http://doi.org/10.5270/S5P-s4ljg54). Data were accessed from the Sentinel-5P Pre-Operations Data Hub (https://s5phub.copernicus.eu/dhus/#/home).

2.3. Ozone lidar

Ozone lidars offer a unique perspective, providing tropospheric ozone profiles at a relatively high temporal and vertical resolution (Gronoff et al., 2019; J. T. Sullivan et al., 2014; John T. Sullivan et al., 2016). The NASA Goddard Space Flight Center (GSFC) Tropospheric Ozone (TROPOZ) Differential Absorption Lidar (DIAL; J. T. Sullivan et al., 2014, 2015) was deployed at the UMBC site and the NASA LaRC Mobile Ozone Lidar (LMOL; De Young et al., 2017; Farris et al., 2019) was located at HMI site. The latter was equipped with a very near field channel that was validated for observing in the 100–1500 m range (Farris et al., 2019). The TROPOZ lidar provided profiles every 10 min with 7 m vertical resolution and the LMOL provided profiles every 10 min with 15 m vertical resolution. These lidars have been previously utilized in other recent campaigns, such as OWLETS in 2017 and Long Island Sound Tropospheric Ozone Study (LISTOS) in 2018, investigating trace gas gradients along land-water interfaces. The accuracy of Tropospheric Ozone Lidar Network (TOLNET) lidars is within 5–10% under both daytime and nighttime conditions (Leblanc et al., 2018; Sullivan et al., 2015; Wang et al., 2017); the network was crucial in standardizing the products, notably the reporting of the uncertainty and the vertical resolution.

2.4. Wind lidar

A Leosphere S200 wind lidar was operated at the HMI site, providing 3D wind speed and direction. The wind speed is derived from 5 consecutive Plan Position Indicator scans using elevation angles 0, 5, 10, 35, and 70°. After grouping data from the 5 scans into fixed altitude bins, the wind direction information can then be derived. These elevation angles were optimized to provide high-resolution wind data at lower altitudes.

2.5. In situ

In situ trace gas measurements were made using existing regulatory sites operated by the Maryland Department of the Environment (MDE) and temporary campaign-specific sites at HMI and UMBC that were operated by various research groups. Each of the fourteen regulatory sites utilized here measured ozone, with some measuring additional trace gases (Table 1). The HMI site measured a large suite of trace gases that was operated by University of Maryland College Park and NOAA Air Resources Laboratory. Additionally, MDE deployed campaign-specific measurements of volatile organic compounds (VOCs) at HMI. For sites that measured ozone, the daily maximum average 8-h (MDA8) ozone was calculated for each day during the campaign to determine if any sites exceeded the National Ambient Air Quality Standard (NAAQS) for ozone. The NAAQS is exceeded when a site measures a MDA8 ozone that is greater than 70 parts per billion (ppbv).

2.6. HYSPLIT

The Hybrid Single-Particle Lagrangian Integrated Trajectory (HYSPLIT) model developed by NOAA Air Resources Laboratory (Stein et al., 2015), was used to run daily back trajectories from the Hart Miller Island site location. The PC Windows-based HYSPLIT v5.0.0 was used to run the trajectories and eventually cluster the daily back trajectory outputs. Daily back trajectories were run 12 h backwards from 18 UTC at 300, 100 and 50 m above ground level (AGL) from June 1 – July 1, 2018. The meteorological input for HYSPLIT was model output from the Weather Research and Forecasting (WRF) model (Skamarock et al., 2008). WRF was run with nested domains of 9, 3, and 1 km horizontal resolution.

Table 1
Trace gas instrument type and sites where the specific instruments were deployed for ozone (upper) and nitrogen dioxide (lower). Asterisks indicates sites that are non-regulatory.

In Situ Ozone (O_3)				
Instrument	Teledyne Model T400	TECO 49C	Thermo 49i	2B Tech Mod. 202
Sites	Aldino, HU Beltsville, Edgewood, Essex, Fairhill, Furley, Glen Burnie, Millington, Oldtown, Padonia, South Carroll	HMI*	UMBC*, EPA Beltsville	Downs Park*, Tolchester*
In Situ Nitrogen Dioxide (NO_2)				
Instrument	**Teledyne T500U**	**LGR Cavity Ring Down**		
Sites	UMBC*	HMI*		

Configuration options followed the model setup described in Ngan and Stein (2017) with the exception that the North American Model (NAM) 12 km was used for initial and boundary conditions instead of the North American Regional Reanalysis (NARR) to utilize high resolution meteorological inputs. The Multi-scale Ultra-high Resolution (MUR) sea surface temperature analysis (1 km horizontal resolution) was used to provide the model high resolution SST values to set the water surface temperature and the convective parameterization was only turned on for the outermost domain. All the HYSPLIT simulations utilized the high resolution 1 km WRF model output. High resolution models are able to better simulate horizontal temperature gradients at land-water gradients and the subsequent bay breeze formation (Loughner et al., 2011), making it an optimal option to investigate the mesoscale meteorological conditions during the OWLETS-2 campaign.

3. Results

3.1. Meteorological background - back trajectory analysis

To initially evaluate the sensitivity of NO_2 and O_3 concentrations and gradients to meteorological variability during the OWLETS-2 intensive operation period (June 2018), HYSPLIT back trajectory modeling was utilized. HYSPLIT back trajectories were run 12 h backwards from 18 UTC at 300, 100, and 50 m above ground level spanning June 1-July 1, 2018. These layers were chosen because the trajectories generally would be within the boundary layer and were altitudes of interest for a case study presented later in this paper. The starting point of the trajectories was the HMI site location to determine the origins of the air that resulted in accumulation of ozone and ozone precursors (e.g., NO_2) over the bay. The 300-m daily back trajectories were then clustered into 5 distinct trajectory clusters based on the total spatial variance (TSV) (https://www.ready.noaa.gov/documents/Tutorial/html/traj_cluseqn.html). When more than 5 clusters were considered, the change in total spatial variance did not change significantly, indicating there was no benefit for utilizing a cluster number greater than five. Based on the days included in each cluster, the 300 (Fig. S2), 100, and 50 m mean trajectories were calculated for each cluster.

Using the final results of the clustering, the mean (Fig. 2, top) and maximum (Fig. 2, middle) of the daily maximum 8-h average (MDA8) ozone was calculated at all sites for all of the days assigned to each cluster. Mean Pandora TC NO_2 were also calculated for all the Pandora instruments (Fig. 2, bottom). Additionally, the frequency of each cluster and the mean and standard deviation of the difference between HMI and UMBC for each cluster was calculated.

Cluster 1's (C1) mean back trajectory shows that air primarily came from areas to the west-southwest of HMI and led to the highest ozone across the study area. The highest ozone values are generally located close to the Baltimore area. This cluster was second most frequent and

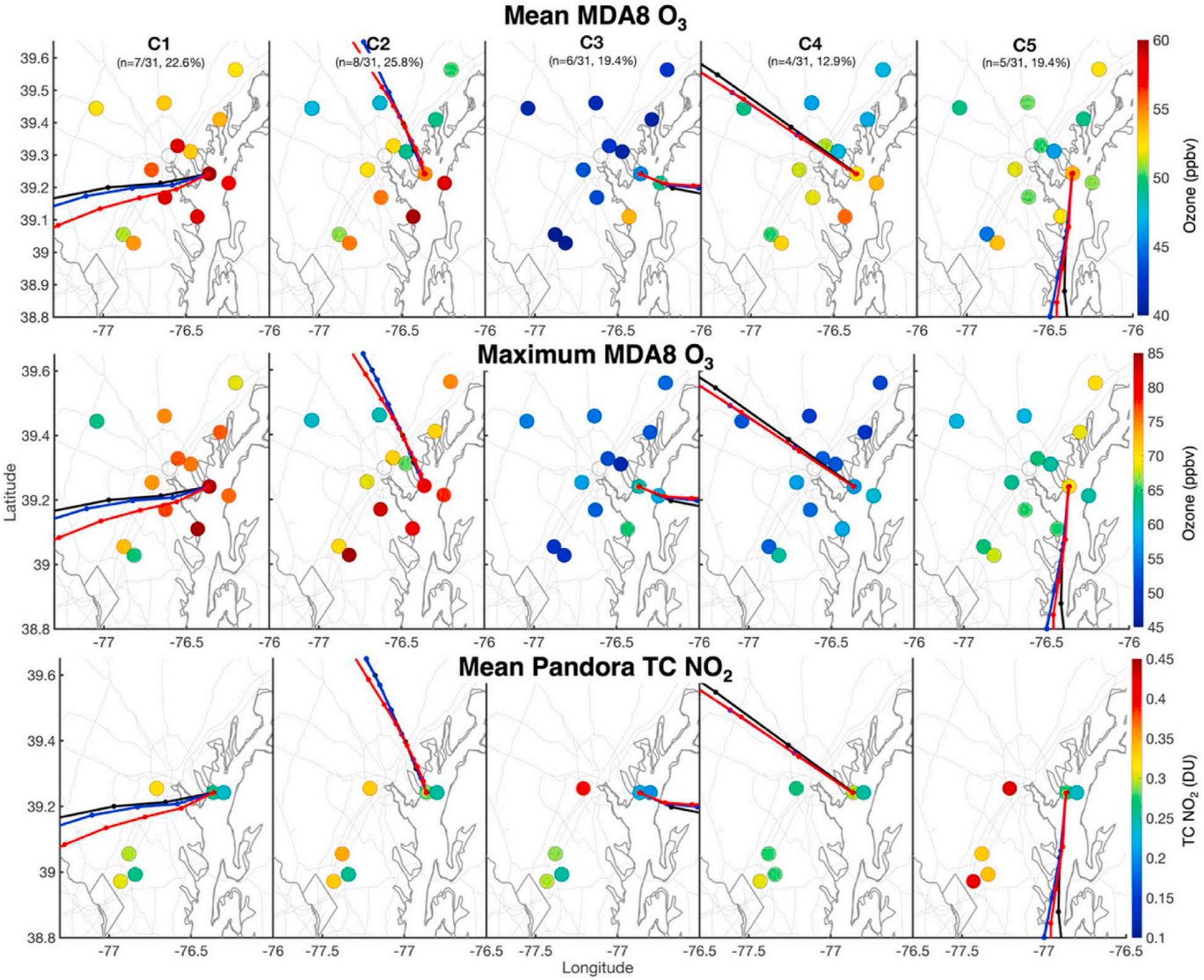

Fig. 2. The mean HYSPLIT 12-h back trajectory for clusters (C#) 1–5 for 300 m (black line), 100 m (blue line), and 50 m (red line). Mean MDA8 (top), maximum MDA8 (middle), and mean Pandora TC NO_2 (bottom) values for each site in each cluster. The frequency of each cluster is noted below the cluster name. Note: the color bar range changes between mean and maximum MDA8 plots. (For interpretation of the references to color in this figure legend, the reader is referred to the Web version of this article.)

resulted in two days where HMI observed higher TC NO_2 than UMBC based on standard deviation.

The mean trajectory for Cluster 2 (C2) was associated with flow from the north-northwest and was the most frequent cluster, occurring ~25% of the time. This cluster had the second highest amount of ozone across the study domain, with coastal sites to the south and east of Baltimore exhibiting the highest values. Sites along the coast (Downs Park and Tolchester, see Fig. 1) and over water (HMI) observed the highest MDA8 ozone values under these conditions. In contrast to C1, which also was associated with high ozone, the mean and maximum MDA8 ozone values in C2 had a noticeable northwest to southeast gradient.

Cluster 3 (C3) featured a back trajectory with easterly flow and had the lowest mean ozone across the domain. The largest positive Pandora TC NO_2 difference was observed between UMBC and HMI when his cluster occurred, meaning that UMBC had consistently larger column NO_2 compared to HMI. Under these conditions, UMBC consistently received air from downtown Baltimore and surrounding interstates, while HMI had air coming from relatively clean, rural areas to the east.

Occurring least frequently, Cluster 4 (C4) was associated with strong northwesterly winds and was responsible for consistently higher TC NO_2 at HMI compared to UMBC. Similar to C3, C4 maximum MDA8 values were in the 50–60 ppbv range, however the mean MDA8 ozone values were notably higher with the highest values on the southern and eastern areas of the Chesapeake Bay.

Cluster 5 (C5) showed an extended period of southerly winds prior to arriving at HMI. The Pandoras at HMI and UMBC observed the largest standard deviation in TC NO_2 when C5 conditions occurred. Interestingly, despite the high ozone observed at HMI during C1 and C2 conditions, HMI also observed elevated mean and max MDA8 ozone compared to all area monitors when C5 occurred.

The HYSPLIT cluster results echo some previously published results by Dreessen et al. (2019) showing that when winds are out of the west (C1) and northwest (C2), ozone concentrations across the study area are typically the highest. C3 conditions demonstrated the cleanest conditions due to relatively low background levels of pollution (both NO_2 and O_3) being transported into the area from the Atlantic. The unique finding from this trajectory analysis, were the impacts observed at HMI under C5 conditions. The highest TC NO_2 was observed across the network of Pandoras when these conditions occurred. Additionally, there was a higher mean and max MDA8 ozone at HMI compared to all area

monitors. Under these weak, southerly winds, transport of ozone precursors over the water translated to some ozone chemistry occurring primarily over water. While the scope of this study concentrated on a 30 day period, future analysis of satellite and ground based measurements should focus on the chemistry over water when these conditions occur.

The variability in the back trajectory clusters additionally demonstrates the non-uniformity between surface ozone and TC NO_2 across the OWLETS-2 domain. To further understand the spatial variability of NO_2 under the various meteorological conditions identified, remotely sensed NO_2 measurements for a multiday ozone event (06/16/18–06/18/18) were analyzed.

3.2. Remote sensing of NO_2 gradients

To quantify the heterogeneity of TC NO_2 during the ozone event, Pandora and TROPOMI observations were analyzed. Daily mean Pandora total column (TC) NO_2 values were calculated for each Pandora site, focusing on detecting gradients between the HMI and UMBC sites. Pandora TC NO_2 median values were also calculated using data ±30 min around the TROPOMI overpass time. Similarly, daily TROPOMI summed total column NO_2 overpass data were extracted for the month of June 2018 for each Pandora site location and were also analyzed spatially.

Due to the unique placement of the HMI site in the Chesapeake Bay, time periods when TC NO_2 was larger over water compared to land were of particular interest. For the majority of the campaign, column NO_2 values measured by TROPOMI and Pandora around overpass times and otherwise (Pandora daily mean), were larger at UMBC compared to HMI (Table 2). HMI has no significant emission sources on the island or in the immediate vicinity, except for Baltimore and industrial sources to the west that only affect the island under specific meteorological conditions. In contrast, the UMBC site is located close to two major highways, I-95 and I-695, both of which are within 1–2 km of the site. Additionally, downtown Baltimore and associated industrial areas are located 8–12 km to the east and southeast of the site.

Based on the proximity to these sources, it was expected that the UMBC site would predominantly observe relatively higher TC NO_2 than HMI. However, there were time periods during the campaign where this pattern was not conserved. On June 16, higher Pandora TC NO_2 was observed at HMI compared to UMBC (Fig. 3) and is further quantified in Table 2. While TC NO_2 was only 0.01–0.03 DU higher at HMI compared to UMBC, capturing this relative enhancement over water at HMI was a significant finding and one of the scientific objectives of the campaign. June 16 was also unique in that it was the first day of the aforementioned ozone event.

Similarly, TROPOMI was also able to spatially capture the accumulation of NO_2 over the Chesapeake Bay on June 16. Fig. 3 shows that in comparison to the June 17 and June 18, there was predominantly higher TC NO_2 over the bay and along the coastlines. This was further quantified (Table 2) by calculating the mean total column NO_2 for pixel centers located within the Chesapeake Bay (Fig. S1). Due to the low spatial resolution of previously available satellite measurements (e.g. OMI), having multiple pixels solely over water to capture accumulation of NO_2 over water was previously not possible. However, with the higher spatial resolution of TROPOMI ($7 \times 3.5\ km^2$), NO_2 gradients were captured spatially and were confirmed by Pandora measurements.

To further examine the meteorological and chemical dynamics closer to ground, surface and column measurements were analyzed with the vertically detailed information provided by the two ozone lidars and a doppler wind lidar.

3.3. Ozone event case study

The June 16–18th, 2018 period consisted of a multi-day ozone event that resulted in two ozone exceedance days and spanned across two weekend-days and one weekday. Not only was there variability in the meteorology across these three days, but there were also distinct differences in the temporal and spatial distributions of surface O_3, surface NO_2, and column NO_2.

For the first day of the ozone event (06/16), the raw 300-m back trajectory showed that the air originated from west of Washington D.C., then curved to the north, following parallel to the western Chesapeake Bay coastline (Fig. 4, left). The 100-m and 50-m back trajectories indicated a different path at the tail end of the trajectory, showing air originating to the south over the central Chesapeake Bay. The overall synoptic pattern featured a weak surface high pressure off the coast of southeast Virginia and an upper level (300 mb) ridge centered over the central Mississippi Valley. The westerly transport overnight at 300 m and southerly transport in the early morning at all trajectory levels suggest pollutants from the Baltimore Washington metropolitan area and central Chesapeake Bay were transported over the bay overnight and into the early morning hours. This day fell into back trajectory Cluster 5, with significant transport from the south and variability in the first 6 h of the trajectory. The last few hours of both the daily (at all levels) and Cluster 5 mean back trajectory, closest to HMI, passed over a heavily industrialized area of Baltimore that includes the third largest NO_x emitter in the state, the Brandon Shores coal fire power plant. Based on the trajectory path, it is probable that NO_x emissions from the Brandon Shores power plant were transported over the HMI site and truly only detectable by remote sensing due to the plume being above the surface. Analysis of the diurnal median Pandora column NO_2 and diurnal mean surface in situ NO_2 at HMI, showed that NO_2 was above the campaign mean during the majority of hours on June 16 (Fig. 5 a, c). Pandora median NO_2 was not only above the campaign mean but was greater than the one standard deviation values at each hour. Despite the Pandora observed accumulation of NO_2 over the Bay at HMI, none of the ozone monitoring sites across the OWLETS-2 domain exceeded on June 16, but the spatial distribution of MDA8 ozone values showed that the three sites located in the northeast of the domain were close to exceeding.

The second day of the ozone event, an exceedance on June 17, was associated with C1, which featured westerly flow towards HMI. While similar to the C1 mean trajectory, the trajectory for June 17 showed westerly flow displaced farther south of the mean, then switching to southerly flow once the trajectory got over the Bay (Fig. 4, middle panel). Similar to the previous day, a weak surface high pressure remained off the coast of southeast Virginia. However, the upper-level ridge at 300 mb moved slightly to the east to be centered over the southeast Great Lakes and surface temperatures were approximately 6° Celsius (10° Fahrenheit) warmer than on June 16. Relatively less TC NO_2 was observed over the Bay by TROPOMI on this day compared to

Table 2
Daily mean Pandora TC NO_2 at HMI and UMBC. Median (±30 min S5P overpass) Pandora TC NO_2 are in the parenthesis.

Date	HMI Pandora TC NO_2 (DU)	UMBC Pandora TC NO_2 (DU)	S5P Overpass Time (UTC)	Chesapeake Bay Mean S5P TC NO_2 (DU)	HMI TROPOMI TC NO_2 (DU)	UMBC TROPOMI TC NO_2 (DU)
06/16	**0.298 (0.276)**	0.268 (0.269)	18:29	**0.235**	**0.284**	0.205
06/17	0.227 (0.199)	**0.340 (0.306)**	18:10	0.213	0.200	**0.227**
06/18	0.286 (0.254)	0.298 (0.288)	17:51	0.203	0.234	–
June 2018	0.256 (0.273)	0.351 (0.385)	–	0.201	0.217	0.222

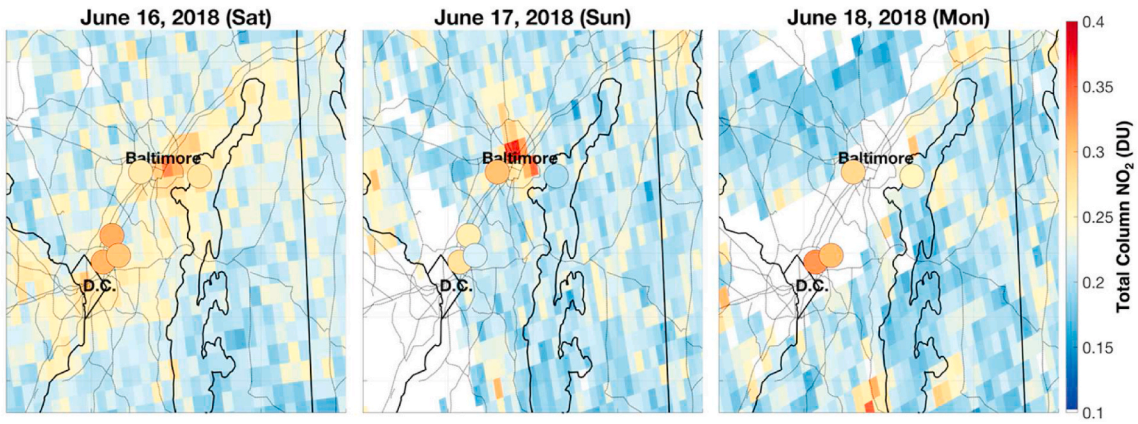

Fig. 3. Daily TROPOMI summed total column NO_2 and median Pandora NO_2 ± 30 min (markers) around the TROPOMI overpass time.

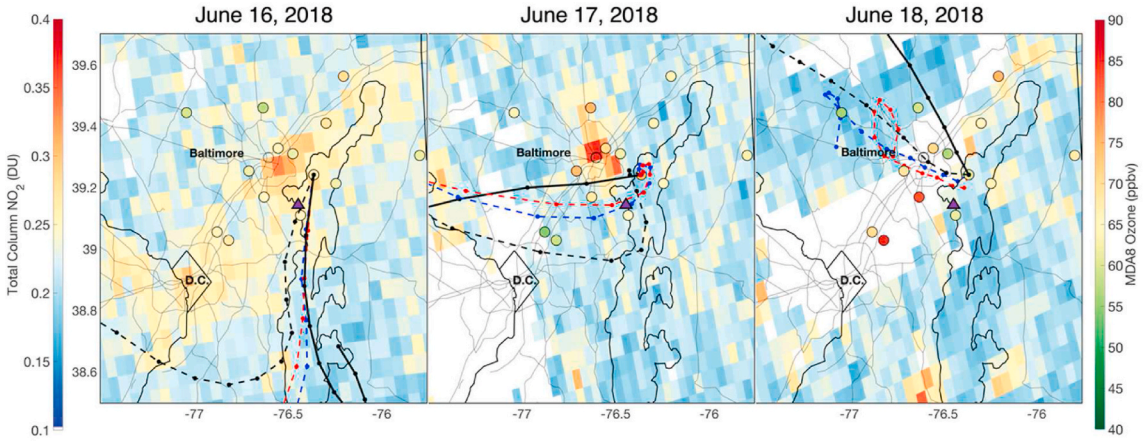

Fig. 4. Daily TROPOMI summed total column NO_2 and MDA8 ozone values (markers) for June 16–18. The date specific cluster mean (solid black line) back trajectory and the original date specific back trajectory at 300 m (dashed black line), 100 m (dashed blue line), and 50 m (dashed red line). The Brandon Shores coal fire power plant is denoted by the purple triangle. (For interpretation of the references to color in this figure legend, the reader is referred to the Web version of this article.)

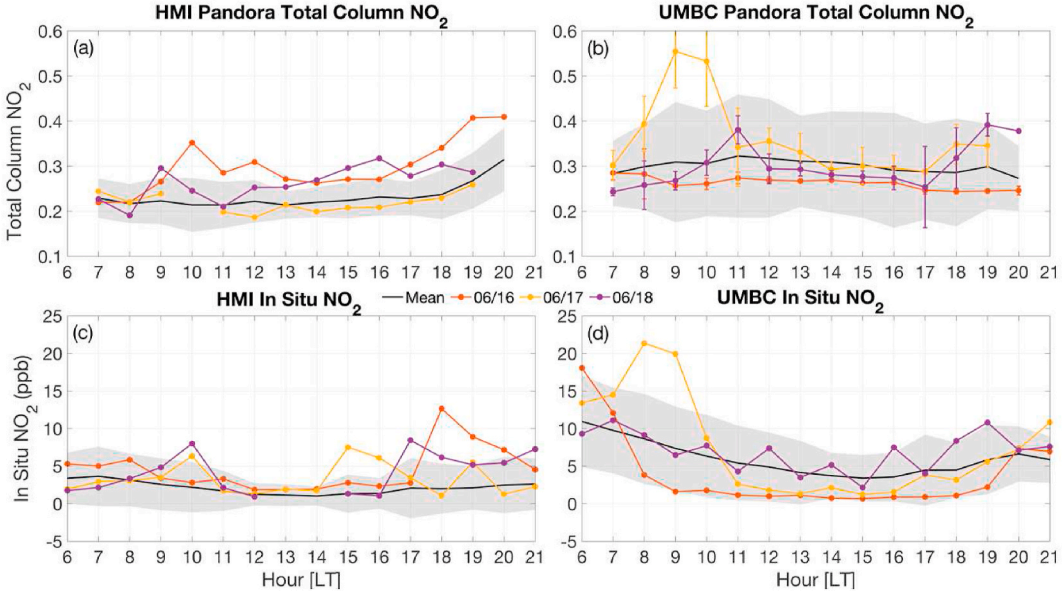

Fig. 5. Hourly median Pandora total column NO_2 amounts for the entire campaign (black solid), June 16 (orange), June 17 (yellow), and June 18 (purple) at HMI (a) and UMBC (b). The same as (a) and (b) except for hourly mean in situ NO_2 at HMI (c) and UMBC (d). (For interpretation of the references to color in this figure legend, the reader is referred to the Web version of this article.)

June 16, with the area of highest TC NO_2 being observed predominately over the downtown Baltimore area (Fig. 4, middle) at overpass time (17:51 UTC). The UMBC site observed coincident increases in Pandora TC NO_2 and in situ surface NO_2 during the morning hours (Fig. 5 b,d), signaling the potential impact of the local morning traffic. This increase in NO_2 in the morning hours was not due to standard rush hour traffic since it was as a Sunday. However, it was Father's Day so there was likely an increase in recreational activity (e.g., boating) leading to NO_x emissions that would not usually be present. Winds were particularly weak on this day indicating that stagnation was occurring across the campaign area. The ozone exceedances on this day were located along and just outside of the I-695 loop around Baltimore metro area, with Padonia having the highest MDA8 ozone concentration. HMI also exceeded the MDA8 ozone standard on this day, despite observing relatively less column (Fig. 5a) and surface NO_2 (Fig. 5c) than the previous day. One factor that may have contributed to ozone production at HMI was the relatively higher VOC concentrations. More specifically, higher concentrations of VOCs emitted from industrial chemical processes (m&p-xylene, toluene) and from mobile gasoline sources (hexane, isopentane1-butene, cyclohexane, 3-methylhexane) were observed on June 17 (Fig. 6). Industrial chemical processing facilities, a large coal fire power plant (e.g. Brandon Shores Coal Fire), and mobile sources (cars, pleasure craft, large container ships, etc.) to the west of HMI are the likely contributors to the VOC make up observed. The VOC measurements added another dimension to this study by providing more insight into the ozone precursors that can be transported to HMI. Distinct species, such as m&p xylene can be linked to specific synthetic chemical manufacturing facilities on the south side of the Baltimore. Additional analysis of the VOCs is beyond the scope of this study, but it is a measurement of high value for further understanding the ozone chemistry over water at HMI.

The last and most significant ozone exceedance day of the event (06/18) fell into C2, which was associated with primarily north-northwesterly flow as indicated by the cluster mean trajectory. The daily back trajectory showed similar behavior, however, was oriented more northwesterly and passing more directly over the downtown Baltimore area. At the surface HMI and UMBC did not observe any consistent surface enhancements of in situ NO_2, except for the afternoon/evening hours at HMI (Fig. 5 c). TC NO_2 measured by Pandora from HMI showed a notable increase around 9 a.m. local time and then consistent enhancements for all of the afternoon hours, while UMBC remained around the mean for the majority of the day. TROPOMI observed cloudier conditions on this day's overpass leading to no valid measurements over the DC Baltimore metropolitan area (Fig. 4, right panel). Elsewhere, TROPOMI observed comparatively higher values of TC NO_2 in northeast Maryland and a section of the eastern shore due east of Baltimore. Meteorologically and chemically, this day was unique compared to the preceding days because of the occurrence of afternoon severe convection and the highest MDA8 ozone values of the three-day event. EPA Beltsville had the highest MDA8 ozone value on this day (85 ppbv) and exceedances occurred in two separate areas. Multiple monitors exceeded in the area between D.C. and Baltimore, with those monitors having the highest MDA8 ozone values. The other area with monitors that exceeded were in northeast Maryland. This day will be further investigated in the next section.

3.4. Vertical O_3 & NO_2 variability

Sharp vertical ozone gradients within the boundary layer are common during the overnight and early morning hours, with the lowest ozone concentrations present closest to the surface where sources of NO_x exist resulting in ozone titration. Ozone concentrations then typically increase with altitude due to the presence of the residual layer, which acts as the storage area for the previous days' ozone. Surface ozone concentrations of approximately 50 ppbv were maintained at HMI for the duration of the nighttime and early morning hours on June 18. This would be consistent with previous work showing that decreased dry deposition velocities (Loughner et al., 2016), reduced cloud cover, and lower boundary layer heights can lead to ozone being 10–20% higher over the Chesapeake Bay compared to coastal monitors (Goldberg et al., 2014). This observation also coincides with previous work by Dreessen et al. (2019), who found overnight/early morning enhancements in surface ozone at HMI compared to nearby land monitors.

Between 4:00–9:00 LT on June 18, surface ozone concentrations were approximately 30–40 ppbv higher at the surface than 150–300 m AGL at HMI. This vertical ozone gradient was unique to HMI (Fig. 7, top) as it was not observed at UMBC (Fig. 7, bottom). To analyze if the relatively lower ozone concentrations in this layer resulted in production of NO_2, the morning HMI Pandora measurements were analyzed. The first Pandora measurements of the day showed relatively elevated

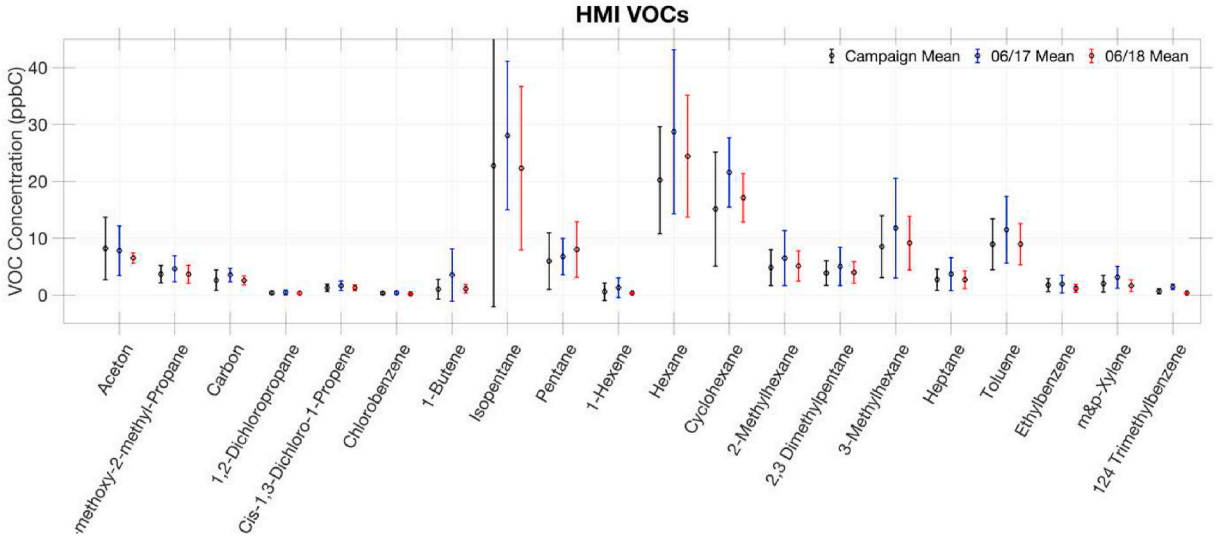

Fig. 6. Daily mean concentrations and standard deviation of select VOCs for 06/17 (blue) and 06/18 (red) at HMI. The campaign mean concentrations and standard deviation of the same VOCs (black). Note that the concentrations are in parts per billion carbon. (For interpretation of the references to color in this figure legend, the reader is referred to the Web version of this article.)

TC NO_2 (~0.25 DU), while surface concentrations did not show any substantial increase or accumulation of NO_2. This suggests that the lofted low ozone concentrations observed by the ozone lidar and the elevated TC NO_2 observed by Pandora, was ozone that was titrated away creating a lofted plume of NO_2, similar to what was observed in OWLETS 2017 (Gronoff et al., 2019). The doppler wind lidar at HMI observed a coincident stratified layer of low wind speeds (Figurer 7, middle) out of the west-southwest, that correlated with the area of lofted low ozone. Complex stratification can occur within marine boundary layers that is driven by stable thermal stability. Within this stratified layer, a plume of NO_x or significantly titrated ozone was transported over HMI and likely originated from one of the industrial sources in and around the Baltimore Harbor based on trajectories.

As morning progressed, significant ozone production was occurring at UMBC with surface concentrations surpassing 70 ppbv by 10:00 LT. HMI did not observe these same surface concentrations, remaining in the 55–65 ppbv range. Between 12:00 and 13:00 UTC, both ozone lidars were observing ozone concentrations aloft of between 90 and 100 ppbv. HMI, in particular, observed a significant increase in ozone between 12:00–12:50 LT. Significant local production or transport over the site were the primary mechanisms causing ozone to increase >40 ppbv over the course of only 50 min. Around 13:00 LT the HMI ozone lidar experienced a power outage resulting in missing data from then through ~17:00 LT. During this time frame thunderstorms began to form in the study area, including a severe thunderstorm that passed over both UMBC and HMI between 15:00 and 17:00 LT. In addition to the presence of thunderstorms, a bay breeze circulation was present. Previous work by Mazzuca et al. (2019) focusing on the DC-Baltimore region, has shown that some of the highest ozone concentrations occur on days when a bay breeze and non-frontal thunderstorms are present. Despite the presence of thunderstorms, UMBC continued to observe >70 ppbv of ozone at the surface. Both ozone lidars did not observe any significant ozone after 17:00 LT, but by that point numerous surface ozone sites had already exceeded the MDA8 ozone standard.

The results of this multiplatform comparison indicated that sharp negative ozone changes with altitude can occur over water. A plume of relatively low ozone observed by the ozone lidar was further corroborated by the Pandora TC NO_2 measurements, which showed enhancements in the TC NO_2 that were not reflected by the surface in situ NO_2 measurements. The ozone lidars and the Pandoras also provided critical insight into the vertical and spatial variability of ozone between land and marine sites on the highest ozone exceedance day of the multiday event.

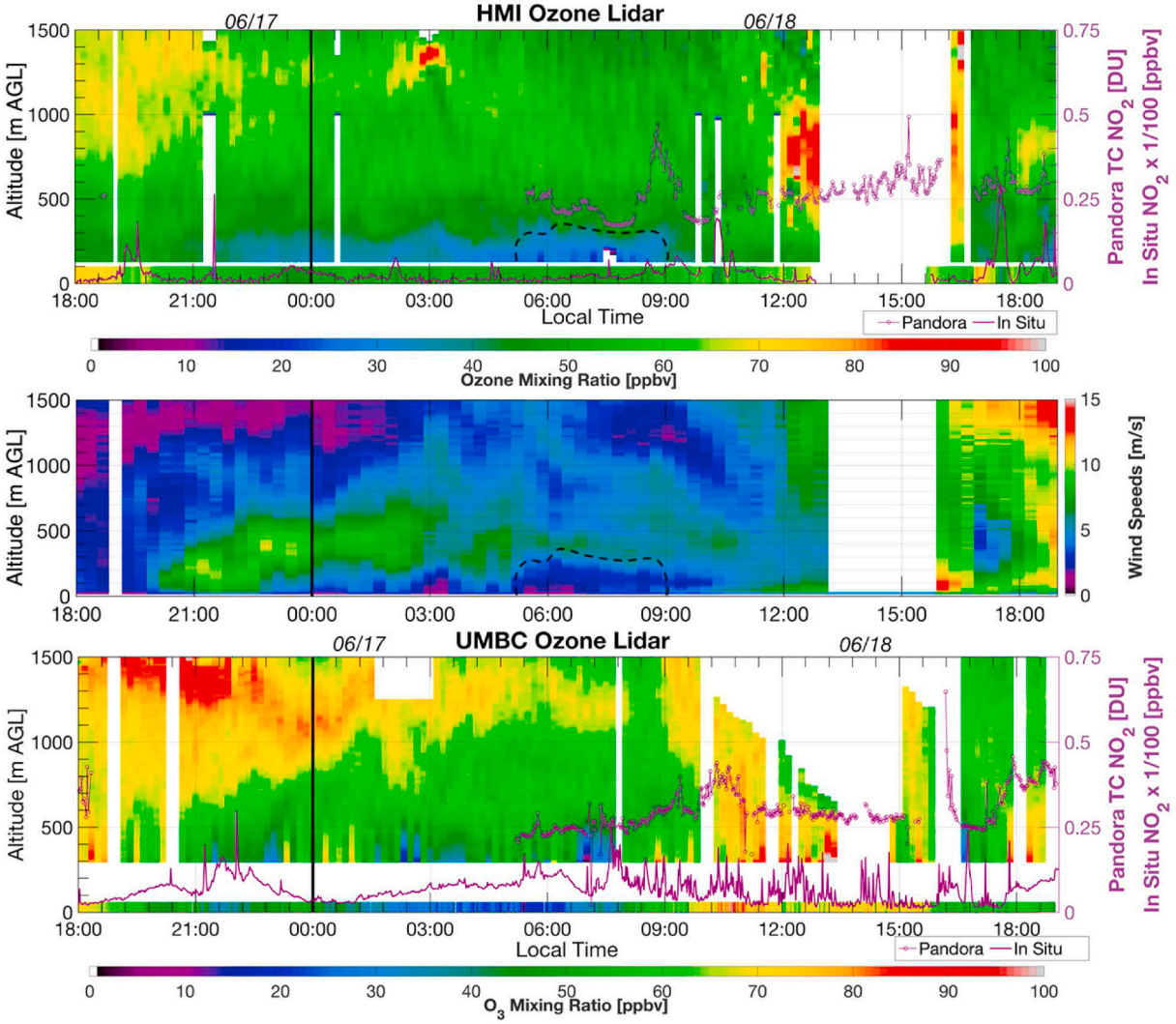

Fig. 7. Top: HMI ozone lidar data in the first 1500 m. Overlaid is the Pandora TC NO_2 (purple line with markers) and the in situ NO_2 (solid purple) concentrations. In situ ozone concentrations are plotted at the base of the plot between 0 and 100 m and shares the same color bar with the ozone lidar data. The location of the titrated ozone layer is shown in the dashed black line. Middle: HMI wind lidar wind speed data in the first 1500 m. Bottom: Same as top but for UMBC. (For interpretation of the references to color in this figure legend, the reader is referred to the Web version of this article.)

4. Conclusions

The lack of columnar and in situ measurements of ozone and ozone precursors over water have made it difficult to fully understand the mechanisms driving ozone pollution at land-water interfaces. The OWLETS-2 field campaign aimed to better quantify the mechanisms affecting the surface, profile and columnar trace gas amounts between the land and water. Using a combination of modeling and a unique set of measurements, these mechanisms were further investigated. High-resolution HYSPLIT model back trajectory simulations were able to effectively capture the small-scale meteorology during the campaign, with the highest ozone concentrations occurring when winds were westerly or northwesterly. A combination of space-based (TROPOMI) and ground-based remote (Pandora) sensing effectively captured the accumulation of NO_2 over the Chesapeake Bay, that was not captured by surface NO_2 measurements. The combination of trajectories and remote sensing measurements allowed for source identification of NO_2 at HMI. In an analysis of a multiday ozone event, significant surface O_3 and NO_2 gradients were found between the land (UMBC) and marine/over water (HMI) sites. The unique configuration of ozone lidar, Pandora, wind lidar, and surface in situ measurements, were able to detect lofted plumes of NO_2 and O_3 over HMI. During the highest ozone day of the multiday event, the ozone lidars captured distinct differences in surface and aloft ozone production. The campaign design during OWLETS-2 and subsequent measurements analyzed in this study have the following broader impactions on future research and regulatory work:

- High-resolution model input (1 km) for trajectory and air quality modeling is necessary for future studies aiming to capture mesoscale influences on pollution transport, especially at land-water interfaces.
- TROPOMI measurements have the spatial resolution and sensitivity to effectively capture NO_2 over water and have been validated by ground truth (Pandora).
- Surface measurements (NO_2 and O_3) can vary significantly from remote sensing measurements (Pandora, TROPOMI, O_3lidar), highlighting the necessity for sensitive profile, columnar, and in situ measurements in complex urban, marine environments.

These observations of O_3 and NO_2 overwater highlight the complexities of pollution transport and chemistry over water. The authors recommend that future air quality investigations in coastal areas collocated in situ, profile (lidars, sondes, etc.), and column measurements (Pandora) at a variety of land and over water sites. The recently established Pandonia Global Network (PGN, https://www.pandonia-global-network.org/), jointly supported by NASA and ESA, is poised to support future efforts by now operationally providing tropospheric NO_2, surface NO_2, and ~0–3 km NO_2 profiles. Leveraging the capabilities of TOLNET (O_3 profiles), PGN (NO_2 profiles), and other ancillary chemical and meteorological measurements will be critical for continued improvement of air quality models and for the future evaluation of geostationary air quality satellite retrievals (e.g. TEMPO).

CRediT authorship contribution statement

Alexander Kotsakis: Conceptualization, Formal analysis, Writing – original draft, Writing – review & editing. **John Sullivan:** Funding acquisition, Data curation, Writing – review & editing. **Thomas Hanisco:** Supervision, Writing – review & editing. **Robert J. Swap:** Supervision, Writing – review & editing. **Vanessa Caicedo:** Data curation, Writing – review & editing. **Tim Berkoff:** Data curation, Writing – review & editing. **Guillaume Gronoff:** Data curation, Writing – review & editing. **Christopher Loughner:** Software, Writing – review & editing. **Xinrong Ren:** Data curation, Writing – review & editing. **Winston Luke:** Data curation. **Paul Kelley:** Data curation. **Phillip R. Stratton:** Data curation. **Ruben Delgado:** Data curation. **Nader Abuhassan:** Data curation. **Lena Shalaby:** Data curation. **Fernando C. Santos:** Data curation, Writing – review & editing. **Joel Dreessen:** Data curation, Writing – review & editing.

Declaration of competing interest

The authors declare that they have no known competing financial interests or personal relationships that could have appeared to influence the work reported in this paper.

Acknowledgements

Dr. Alexander Kotsakis's research was supported by an appointment to the NASA Postdoctoral Program at the Goddard Space Flight Center Atmospheric Chemistry and Dynamics Laboratory administered by Universities Space Research Association under contract with NASA. Unless otherwise noted, all data from the OWLETS-2 campaign and those used in this manuscript have been uploaded to an archive web interface (www air.larc.nasa.gov/missions/owlets). Additional field reports, flight forecasts, presentations, and other information to facilitate use of OWLETS-2 data by the research community at large. The 1 km WRF output used for the HYSPLIT trajectory modeling was provided by Christopher Loughner and is available through the NOAA Air Resources Laboratory (ftp://arlftp.arlhq.noaa.gov/pub/archives/owlets2/). The authors gratefully acknowledge support provided by the NASA/ESA Pandonia Global Network (PGN), Tropospheric Ozone Lidar Network (TOLNet), and the NASA Tropospheric Chemistry Program.

Appendix A. Supplementary data

Supplementary data to this article can be found online at https://doi.org/10.1016/j.atmosenv.2022.119063.

References

Avnery, S., Mauzerall, D.L., Liu, J., Horowitz, L.W., 2011. Global crop yield reductions due to surface ozone exposure: 2. Year 2030 potential crop production losses and economic damage under two scenarios of O3 pollution. Atmos. Environ. 45 (13), 2297–2309. https://doi.org/10.1016/j.atmosenv.2011.01.002.

Banta, R.M., Senff, C.J., Alvarez, R.J., Langford, A.O., Parrish, D.D., Trainer, M.K., Darby, L.S., Michael Hardesty, R., Lambeth, B., Andrew Neuman, J., Angevine, W. M., Nielsen-Gammon, J., Sandberg, S.P., White, A.B., 2011. Dependence of daily peak O3 concentrations near Houston, Texas on environmental factors: wind speed, temperature, and boundary-layer depth. Atmos. Environ. 45 (1), 162–173. https://doi.org/10.1016/j.atmosenv.2010.09.030.

Banta, R.M., Senff, C.J., Nielsen-Gammon, J., Darby, L.S., Ryerson, T.B., Alvarez, R.J., Sandberg, S.R., Williams, E.J., Trainer, M., 2005. A bad air day in Houston. Bull. Am. Meteorol. Soc. 86 (5), 657–669. https://doi.org/10.1175/BAMS-86-5-657.

Boersma, K.F., Eskes, H.J., Brinksma, E.J., 2004. Error analysis for tropospheric NO2 retrieval from space. J. Geophys. Res. Atmos. 109 (4), 4311. https://doi.org/10.1029/2003jd003962.

Caicedo, V., Rappenglueck, B., Cuchiara, G., Flynn, J., Ferrare, R., Scarino, A.J., Berkoff, T., Senff, C., Langford, A., Lefer, B., 2019. Bay breeze and sea breeze circulation impacts on the planetary boundary layer and air quality from an observed and modeled DISCOVER-AQ Texas case study. J. Geophys. Res. Atmos. 124 (13) https://doi.org/10.1029/2019JD030523, 2019JD030523.

Cede, A., 2021. Pandonia Global Network Data Products Readme Document Version 1.8-3 available at: https://www.pandonia-global-network.org/wp-content/uploads/2021/01/PGN_DataProducts_Readme_v1-8-3.pdf. (Accessed 15 March 2021).

Cede, A., 2019. Manual for Blick Software Suite 1.7, Version 7 available at: https://www.pandonia-global-network.org/wp-content/uploads/2019/11/BlickSoftwareSuite_Manual_v1-7.pdf. (Accessed 15 March 2021).

De Young, R., Carrion, W., Ganoe, R., Pliutau, D., Gronoff, G., Berkoff, T., Kuang, S., 2017. Langley mobile ozone lidar: ozone and aerosol atmospheric profiling for air quality research. Appl. Opt. 56 (3), 721. https://doi.org/10.1364/ao.56.000721.

Dreessen, J., Orozco, D., Boyle, J., Szymborski, J., Lee, P., Flores, A., Sakai, R.K., 2019. Observed ozone over the Chesapeake bay land-water interface: the Hart-Miller island pilot project. J. Air Waste Manag. Assoc. 69 (11), 1312–1330. https://doi.org/10.1080/10962247.2019.1668497.

Farris, B.M., Gronoff, G.P., Carrion, W., Knepp, T., Pippin, M., Berkoff, T.A., 2019. Demonstration of an off-Axis parabolic receiver for near-range retrieval of lidar ozone profiles. Atmos. Meas. Tech. 12 (1), 363–370. https://doi.org/10.5194/amt-12-363-2019.

Fishman, J., Bowman, K.W., Burrows, J.P., Richter, A., Chance, K.V., Edwards, D.P., Martin, R.V., Morris, G.A., Pierce, R.B., Ziemke, J.R., Al-Saadi, J.A., Creilson, J.K., Schaack, T.K., Thompson, A.M., 2008. Remote sensing of tropospheric pollution from space. In: Bulletin of the American Meteorological Society, vol. 89. American

Meteorological Society, pp. 805–821. https://doi.org/10.1175/2008BAMS2526.1, 6.
Flynn, C.M., Pickering, K.E., Crawford, J.H., Weinheimer, A.J., Diskin, G., Thornhill, K. L., Loughner, C., Lee, P., Strode, S.A., 2016. Variability of O3 and NO2 profile shapes during DISCOVER-AQ: implications for satellite observations and comparisons to model-simulated profiles. Atmos. Environ. 147, 133–156. https://doi.org/10.1016/j.atmosenv.2016.09.068.
Goldberg, D.L., Lamsal, L.N., Loughner, C.P., Swartz, W.H., Lu, Z., Streets, D.G., 2017. A high-resolution and observationally constrained OMI NO 2 satellite retrieval. Atmos. Chem. Phys. 17, 11403–11421. https://doi.org/10.5194/acp-17-11403-2017.
Goldberg, D.L., Loughner, C.P., Tzortziou, M., Stehr, J.W., Pickering, K.E., Marufu, L.T., Dickerson, R.R., 2014. Higher surface ozone concentrations over the Chesapeake Bay than over the adjacent land: observations and models from the DISCOVER-AQ and CBODAQ campaigns. Atmos. Environ. 84, 9–19. https://doi.org/10.1016/j.atmosenv.2013.11.008.
Griffin, D., Zhao, X., McLinden, C.A., Boersma, F., Bourassa, A., Dammers, E., Degenstein, D., Eskes, H., Fehr, L., Fioletov, V., Hayden, K., Kharol, S.K., Li, S.M., Makar, P., Martin, R.V., Mihele, C., Mittermeier, R.L., Krotkov, N., Sneep, M., Wolde, M., 2019. High-resolution mapping of nitrogen dioxide with TROPOMI: first results and validation over the Canadian oil sands. Geophys. Res. Lett. 46 (2), 1049–1060. https://doi.org/10.1029/2018GL081095.
Gronoff, G., Robinson, J., Berkoff, T., Swap, R., Farris, B., Schroeder, J., Halliday, H.S., Knepp, T., Spinei, E., Carrion, W., Adcock, E.E., Johns, Z., Allen, D., Pippin, M., 2019. A method for quantifying near range point source induced O3 titration events using Co-located Lidar and Pandora measurements. Atmos. Environ. 204, 43–52. https://doi.org/10.1016/j.atmosenv.2019.01.052.
He, H., Loughner, C.P., Stehr, J.W., Arkinson, H.L., Brent, L.C., Follette-Cook, M.B., Tzortziou, M.A., Pickering, K.E., Thompson, A.M., Martins, D.K., Diskin, G.S., Anderson, B.E., Crawford, J.H., Weinheimer, A.J., Lee, P., Hains, J.C., Dickerson, R. R., 2013. An elevated reservoir of air pollutants over the Mid-Atlantic States during the 2011 DISCOVER-AQ campaign: airborne measurements and numerical simulations. Atmos. Environ. 85, 18–30. https://doi.org/10.1016/j.atmosenv.2013.11.039.
Herman, J., Cede, A., Spinei, E., Mount, G., Tzortziou, M., Abuhassan, N., 2009. NO2 column amounts from ground-based Pandora and MFDOAS spectrometers using the direct-sun DOAS technique: intercomparisons and application to OMI validation. J. Geophys. Res. Atmos. 114 (13) https://doi.org/10.1029/2009jd011848.
Herman, J.R., Spinei, E., Fried, A., Kim, Jhoon, Kim, Jae, Kim, W., Cede, A., Abuhassan, N.K., Segal-Rozenhaimer, M., 2018. NO2 and HCHO measurements in Korea from 2012 to 2016 from Pandora spectrometer instruments compared with OMI retrievals and with aircraft measurements during the KORUS-AQ campaign. Atmos. Meas. Tech. 11, 4583–4603. https://doi.org/10.5194/amt-11-4583-2018.
Ialongo, I., Virta, H., Eskes, H., Hovila, J., Douros, J., 2020. Comparison of TROPOMI/Sentinel-5 Precursor NO2 observations with ground-based measurements in Helsinki. Atmos. Meas. Tech. 13 (1), 205–218. https://doi.org/10.5194/amt-13-205-2020.
Judd, L.M., Al-Saadi, J.A., Janz, S.J., Kowalewski, M.G., Pierce, R.B., Szykman, J.J., Valin, L.C., Swap, R., Cede, A., Mueller, M., Tiefengraber, M., Abuhassan, N., Williams, D., 2019. Evaluating the impact of spatial resolution on tropospheric NO& lt;sub& gt;2& lt;/sub& gt; column comparisons within urban areas using high-resolution airborne data. Atmos. Meas. Tech. 12 (11), 6091–6111. https://doi.org/10.5194/amt-12-6091-2019.
Kim, H.C., Lee, P., Judd, L.M., Pan, L., Lefer, B.L., 2016. OMI NO2 column densities over North American urban cities: the effect of satellite footprint resolution. Geosci. Model Dev. (GMD) 9, 1111–1123. https://doi.org/10.5194/gmd-9-1111-2016.
Knepp, T., Pippin, M., Crawford, J., Chen, G., Szykman, J., Long, R., Cowen, L., Cede, A., Abuhassan, N., Herman, J., Delgado, R., Compton, J., Berkoff, T., Fishman, J., Martins, D., Stauffer, R., Thompson, A.M., Weinheimer, A., Knapp, D., Neil, D., 2015. Estimating surface NO2 and SO2 mixing ratios from fast-response total column observations and potential application to geostationary missions. J. Atmos. Chem. 72 (3–4), 261–286. https://doi.org/10.1007/s10874-013-9257-6.
Lamsal, L.N., Krotkov, N.A., Celarier, E.A., Swartz, W.H., Pickering, K.E., Bucsela, E.J., Gleason, J.F., Martin, R.V., Philip, S., Irie, H., Cede, A., Herman, J., Weinheimer, A., Szykman, J.J., Knepp, T.N., 2014. Evaluation of OMI operational standard NO 2 column retrievals using in situ and surface-based NO 2 observations. Atmos. Chem. Phys. 14, 11587–11609. https://doi.org/10.5194/acp-14-11587-2014.
Leblanc, T., Brewer, M.A., Wang, P.S., Jose Granados-Muñoz, M., Strawbridge, K.B., Travis, M., Firanski, B., Sullivan, J.T., McGee, T.J., Sumnicht, G.K., Twigg, L.W., Berkoff, T.A., Carrion, W., Gronoff, G., Aknan, A., Chen, G., Alvarez, R.J., Langford, A.O., Senff, C.J., Newchurch, M.J., 2018. Validation of the TOLNet lidars: the southern California ozone observation Project (SCOOP). Atmos. Meas. Tech. 11 (11), 6137–6162. https://doi.org/10.5194/amt-11-6137-2018.
Lefohn, A.S., Foley, J.K., 1993. Establishing relevant ozone standards to protect vegetation and human health: exposure dose-response considerations. Air Waste 43 (1), 106–112. https://doi.org/10.1080/1073161X.1993.10467111.
Li, W., Wang, Y., Bernier, C., Estes, M., 2020. Identification of sea breeze recirculation and its effects on ozone in Houston, TX, during DISCOVER-AQ 2013. J. Geophys. Res. Atmos. 125 (22), e2020JD033165 https://doi.org/10.1029/2020JD033165.
Lorente, A., Folkert Boersma, K., Yu, H., Dörner, S., Hilboll, A., Richter, A., Liu, M., Lamsal, L.N., Barkley, M., De Smedt, I., Van Roozendael, M., Wang, Y., Wagner, T., Beirle, S., Lin, J.T., Krotkov, N., Stammes, P., Wang, P., Eskes, H.J., Krol, M., 2017. Structural uncertainty in air mass factor calculation for NO2 and HCHO satellite retrievals. Atmos. Meas. Tech. 10 (3), 759–782. https://doi.org/10.5194/amt-10-759-2017.
Loughner, C.P., Allen, D.J., Pickering, K.E., Zhang, D.L., Shou, Y.X., Dickerson, R.R., 2011. Impact of fair-weather cumulus clouds and the Chesapeake Bay breeze on pollutant transport and transformation. Atmos. Environ. 45 (24), 4060–4072. https://doi.org/10.1016/j.atmosenv.2011.04.003.
Loughner, C.P., Tzortziou, M., Follette-Cook, M., Pickering, K.E., Goldberg, D., Satam, C., Weinheimer, A., Crawford, J.H., Knapp, D.J., Montzka, D.D., Diskin, G.S., Dickerson, R.R., 2014. Impact of bay-breeze circulations on surface air quality and boundary layer export. J. Appl. Meteorol. Climatol. 53 (7), 1697–1713. https://doi.org/10.1175/JAMC-D-13-0323.1.
Loughner, C.P., Tzortziou, M., Shroder, S., Pickering, K.E., 2016. Enhanced dry deposition of nitrogen pollution near coastlines: A case study covering the Chesapeake Bay Estuary and Atlantic Ocean Coastline. J. Geophys. Res. Atmos. 121 (23), 14221–14238. https://doi.org/10.1002/2016jd025571.
Mazzuca, G.M., Pickering, K.E., New, D.A., Dreessen, J., Dickerson, R.R., 2019. Impact of bay breeze and thunderstorm circulations on surface ozone at a site along the Chesapeake Bay 2011-2016. Atmos. Environ. 198, 351–365. https://doi.org/10.1016/j. atmosenv.2018.10.068.
Ngan, F., Stein, A.F., 2017. A long-term WRF meteorological archive for dispersion simulations: application to controlled tracer experiments. J. Appl. Meteorol. Climatol. 56 (8), 2203–2220. https://journals.ametsoc.org/view/journals/apme/56/8/jamc-d-16-0345.1.xml.
Peel, J.L., Tolbert, P.E., Klein, M., Metzger, K.B., Flanders, W.D., Todd, K., Mulholland, J. A., Ryan, P.B., Frumkin, H., 2005. Ambient air pollution and respiratory emergency department visits. Epidemiology 16 (2), 164–174. https://doi.org/10.1097/01.ede.0000152905.42113.db.
Rappenglück, B., Perna, R., Zhong, S., Morris, G.A., 2008. An analysis of the vertical structure of the atmosphere and the upper-level meteorology and their impact on surface ozone levels in Houston, Texas. J. Geophys. Res. Atmos. 113 (17) https://doi.org/10.1029/2007JD009745.
Ryu, Y.H., Baik, J.J., Kwak, K.H., Kim, S., Moon, N., 2013. Impacts of urban land-surface forcing on ozone air quality in the Seoul metropolitan area. Atmos. Chem. Phys. 13 (4), 2177–2194. https://doi.org/10.5194/acp-13-2177-2013.
Skamarock, W.C., Klemp, J.B., Dudhia, J., Gill, D.O., Barker, D.M., Wang, W., Powers, J. G., 2008. A Description of the Advanced Research WRF Version 3. *NCAR Technical note -475+STR*.
Solomon, S., 1999. Stratospheric ozone depletion: a review of concepts and history. In: Reviews of Geophysics, vol. 37. Blackwell Publishing Ltd, pp. 275–316. https://doi.org/10.1029/1999RG900008, 3.
Stauffer, R.M., Thompson, A.M., Martins, D.K., Clark, R.D., Goldberg, D.L., Loughner, C. P., Delgado, R., Dickerson, R.R., Stehr, J.W., Tzortziou, M.A., 2015. Bay breeze influence on surface ozone at Edgewood, MD during July 2011. J. Atmos. Chem. 72 (3–4), 335–353. https://doi.org/10.1007/s10874-012-9241-6.
Stein, A.F., Draxler, R.R., Rolph, G.D., Stunder, B.J.B., Cohen, M.D., Ngan, F., 2015. Noaa's hysplit atmospheric transport and dispersion modeling system. In: Bulletin of the American Meteorological Society, vol. 96. American Meteorological Society, pp. 2059–2077. https://doi.org/10.1175/BAMS-D-14-00110.1, 12.
Sullivan, J.T., McGee, T.J., Leblanc, T., Sumnicht, G.K., Twigg, L.W., 2015. Optimization of the GSFC TROPOZ DIAL retrieval using synthetic lidar returns and ozonesondes - Part 1: algorithm validation. Atmos. Meas. Tech. 8 (10), 4133–4143. https://doi.org/10.5194/amt-8-4133-2015.
Sullivan, J.T., McGee, T.J., Sumnicht, G.K., Twigg, L.W., Hoff, R.M., 2014. A mobile differential absorption lidar to measure sub-hourly fluctuation of tropospheric ozone profiles in the Baltimore-Washington, D.C. region. Atmos. Meas. Tech. 7 (10), 3529–3548. https://doi.org/10.5194/amt-7-3529-2014.
Sullivan, John T., Berkoff, T., Gronoff, G., Knepp, T., Pippin, M., Allen, D., Twigg, L., Swap, R., Tzortziou, M., Thompson, A.M., Stauffer, R.M., Wolfe, G.M., Flynn, J., Pusede, S.E., Judd, L.M., Moore, W., Baker, B.D., Al-Saadi, J., Mcgee, T.J., 2019. The ozone water-land environmental transition study: an innovative strategy for understanding Chesapeake Bay pollution events. Bull. Am. Meteorol. Soc. 100 (2), 291–306. https://doi.org/10.1175/BAMS-D-18-0025.1.
Sullivan, John T., McGee, T.J., DeYoung, R., Twigg, L.W., Sumnicht, G.K., Pliutau, D., Knepp, T., Carrion, W., 2015. Results from the NASA GSFC and LaRC Ozone Lidar intercomparison: new mobile tools for atmospheric research. J. Atmos. Ocean. Technol. 32 (10), 1779–1795. https://doi.org/10.1175/JTECH-D-14-00193.1.
Sullivan, John T., McGee, T.J., Langford, A.O., Alvarez, R.J., Senff, C.J., Reddy, P.J., Thompson, A.M., Twigg, L.W., Sumnicht, G.K., Lee, P., Weinheimer, A., Knote, C., Long, R.W., Hoff, R.M., 2016. Quantifying the contribution of thermally driven recirculation to a high-ozone event along the Colorado Front Range using lidar. J. Geophys. Res. 121 (17), 10377–10390. https://doi.org/10.1002/2016JD025229.
Sullivan, John T., Rabenhorst, S.D., Dreessen, J., McGee, T.J., Delgado, R., Twigg, L., Sumnicht, G., 2017. Lidar observations revealing transport of O3 in the presence of a nocturnal low-level jet: Regional implications for "next-day" pollution. Atmos. Environ. 158, 160–171. https://doi.org/10.1016/j.atmosenv.2017.03.039.
Wang, L., Newchurch, M.J., Alvarez, R.J., Berkoff, T.A., Brown, S.S., Carrion, W., De Young, R.J., Johnson, B.J., Ganoe, R., Gronoff, G., Kirgis, G., Kuang, S., Langford, A. O., Leblanc, T., McDuffie, E.E., McGee, T.J., Pliutau, D., Senff, C.J., Sullivan, J.T., Weinheimer, A.J., 2017. Quantifying TOLNet ozone lidar accuracy during the 2014 DISCOVER-AQ and FRAPPÉ campaigns. Atmos. Meas. Tech. 10 (10), 3865–3876. https://doi.org/10.5194/amt-10-3865-2017.
Williams, J.E., Folkert Boersma, K., Le Sager, P., Verstraeten, W.W., 2017. The high-resolution version of TM5-MP for optimized satellite retrievals: description and validation. Geosci. Model Dev. (GMD) 10 (2), 721–750. https://doi.org/10.5194/gmd-10-721-2017.
Zhang, J., Ninneman, M., Joseph, E., Schwab, M.J., Shrestha, B., Schwab, J.J., 2020. Mobile laboratory measurements of high surface ozone levels and spatial

heterogeneity during LISTOS 2018: evidence for sea breeze influence. J. Geophys. Res. Atmos. 125 (11), e2019JD031961 https://doi.org/10.1029/2019JD031961.
Zhang, Y., Wang, Y., Chen, G., Smeltzer, C., Crawford, J., Olson, J., Szykman, J., Weinheimer, A.J., Knapp, D.J., Montzka, D.D., Wisthaler, A., Mikoviny, T., Fried, A., Diskin, G., 2016. Large vertical gradient of reactive nitrogen oxides in the boundary layer: modeling analysis of DISCOVER-AQ 2011 observations. J. Geophys. Res. Atmos. 121 (4), 1922–1934. https://doi.org/10.1002/2015JD024203.
Zhao, X., Griffin, D., Fioletov, V., Mclinden, C., Cede, A., Tiefengraber, M., Müller, M., Bognar, K., Strong, K., Boersma, F., Eskes, H., Davies, J., Ogyu, A., Lee, S.C., 2020. Assessment of the quality of TROPOMI high-spatial-resolution NO 2 data products in the Greater Toronto Area. Atmos. Meas. Tech. 13, 2131–2159. https://doi.org/10.5194/amt-13-2131-2020.
Zoogman, P., Liu, X., Suleiman, R.M., Pennington, W.F., Flittner, D.E., Al-Saadi, J.A., Hilton, B.B., Nicks, D.K., Newchurch, M.J., Carr, J.L., Janz, S.J., Andraschko, M.R., Arola, A., Baker, B.D., Canova, B.P., Chan Miller, C., Cohen, R.C., Davis, J.E., Dussault, M.E., Chance, K., 2017. Tropospheric emissions: monitoring of pollution (TEMPO). In: Journal of Quantitative Spectroscopy and Radiative Transfer, vol. 186. Elsevier Ltd, pp. 17–39. https://doi.org/10.1016/j.jqsrt.2016.05.008.